

# A Counterexample to Claimed COBE Constraints on Compact Toroidal Universe Models

Boudewijn F. Roukema  
 Inter-University Centre for Astronomy and Astrophysics  
 Post Bag 4, Ganeshkhind, Pune, 411 007, India  
 Email: boud@iucaa.ernet.in

Le 30 octobre 2018

## Abstract

It has been suggested that if the Universe satisfies a flat, multiply connected, perturbed Friedmann-Lemaître model, then cosmic microwave background data from the COBE satellite implies that the minimum size of the injectivity diameter (shortest closed spatial geodesic) must be larger than about two fifths of the horizon diameter. To show that this claim is misleading, a simple  $T^2 \times R$  universe model of injectivity diameter a quarter of this size, i.e. a tenth of the horizon diameter, is shown to be consistent with COBE four year observational maps of the cosmic microwave background. This is done using the identified circles principle.

*PACS numbers:* 98.80.Es, 04.20.Gz, 02.40.-k, 98.54.-h

## 1 Introduction

Since Schwarzschild's (1900; 1998) 'few remarks' which required 'a total break with the astronomers' deeply entrenched views' of zero curvature and trivial topology at the beginning of the twentieth century, observational research into cosmic topology progressed very slowly until 1993. In that year, a burst of articles comparing special cases or classes of multiply connected models with observations of the cosmic microwave background (CMB) by the COBE satellite (Stevens et al. 1993; Sokolov 1993; Starobinsky 1993; Fang 1993; Jing & Fang 1994) were published, followed by the review article of Lachièze-Rey & Luminet (1995) and new or updated (topology independent) methods of analysing three-dimensional catalogues of conventional astrophysical objects (Lehoucq et al. 1996; Roukema 1996; Roukema & Edge 1997) were

also invented.

Further work in analysing COBE data has been carried out, both for flat (de Oliveira Costa & Smoot 1995; de Oliveira-Costa et al. 1996; Levin et al. 1998) and for hyperbolic (Bond et al. 1998; Inoue 1999; Aurich 1999; Cornish & Spergel 1999) multiply connected models.

The COBE analyses simulate structure in the Universe for given 3-manifolds and estimate the probability that statistical properties of the observed CMB temperature fluctuations could have been drawn from distributions of those same properties for the simulated structures. This is useful work, but requires assumptions which are likely to be somewhat modified in the case that the Universe is observably compact, and results in statements which may relate more to the assumed probability distributions representing structure than to the statistics of measurement uncertainty [e.g. Section 1.2 of Roukema (2000) or Sect. 5.3.2(ii) of Luminet & Roukema (1999)].

A more direct observational approach is simply to test the self-consistency of the CMB temperature fluctuations with the multiple topological imaging implied by any hypothesised multiply connected model. The exact set of points which should be multiply imaged consists of a set of identified circles on the surface of last scattering (Cornish, Spergel & Starkman 1996, 1998b; Weeks 1998). Given the measurement uncertainties in the temperature fluctuations, a model can be treated as a null hypothesis which one tries to reject. If hypothetically corresponding sky pixels do not have significantly different temperatures, then the model is consistent with the data.

This approach avoids the risk of assuming perturbation statistics which could be inconsistent with the hypothesis being tested. An applica-

tion of the identified circles principle to COBE data has previously been demonstrated on an observationally motivated toroidal universe model in Roukema (2000).

In this paper, a small value of the injectivity diameter,  $2r_{\text{inj}} \equiv 2R_H/10$  (where  $R_H$  is the horizon radius), is chosen, likely possibilities for the optimal orientations for a ‘2-torus’ ( $T^2 \times R$  model, hereafter ‘ $T^2$ ’) are found based on the four year COBE DMR data, and its consistency within measurement error of the four year COBE DMR data is examined. To avoid confusion by non-specialist readers, it is noted here that for a flat, zero cosmological constant model, the horizon radius in comoving coordinates is  $R_H = 2c/H_0 = 6000h^{-1}$  Mpc, so that  $0.8R_H = 0.4(2R_H) = 4800h^{-1}$  Mpc and  $2R_H/10 = 1200h^{-1}$  Mpc.

The constraints suggested by authors such as Stevens et al. (1993), Levin et al. (1998) are that  $2r_{\text{inj}} > 8R_H/10$ . A counterexample with  $2r_{\text{inj}} = 2R_H/10$  is clearly sufficient to disprove the suggested constraints.

The assumption regarding structure formation common to other authors’ work (cited above), i.e. that the temperature fluctuations are due to the naïve Sachs-Wolfe effect (Sachs & Wolfe 1967), is adopted here, but complemented by consideration of the integrated Sachs-Wolfe effect (Sachs & Wolfe 1967) (hereafter, NSW and ISW, respectively) which the above authors did not quantitatively consider [though see, e.g. Cornish, Spergel & Starkman (1998a,b), Uzan (1998), for order of magnitude arguments regarding the relevance of the ISW for cosmic topology]. The ISW is expected to be significant at COBE scales for flat models with a non-zero value of the cosmological constant (e.g. White et al. 1994; Crittenden & Turok 1996), though not as large as it would be for hyperbolic models of corresponding matter densities  $\Omega_0$ . Given the recent observational evidence in favour of a flat, cosmological constant dominated universe (Fukugita et al. 1990; Fort et al. 1997; Chiba & Yoshii 1997; Perlmutter et al. 1999), observational motivation for considering the ISW also exists.

The method is defined in Sect. 2, the observational data are described in Sect. 2.5, the results are presented in Sect. 3 and further discussion is provided in Sect. 4.

For reviews on cosmological topology, see Lachièze-Rey & Luminet (1995), Luminet (1998), Starkman (1998) and Luminet & Roukema (1999).

For workshop proceedings on the subject, see Starkman (1998) and following articles, and Blançœil & Roukema (1999). For a list and discussion of both two-dimensional and three-dimensional methods, see Table 2 of Luminet & Roukema (1999) and the accompanying discussion. The reader should be reminded that rapid development in the three-dimensional methods is presently being carried out (Lehoucq et al. 1996; Roukema 1996; Fagundes & Gausmann 1998; Roukema & Edge 1997; Roukema & Blançœil 1998; Gomero et al. 1999a; Lehoucq et al. 1999; Fagundes & Gausmann 1999a; Uzan et al. 1999; Fagundes & Gausmann 1999b; Gomero et al. 1999b,c).

The Hubble constant is parametrised here as  $h \equiv H_0/100 \text{ km s}^{-1} \text{ Mpc}^{-1}$ . Comoving coordinates are used (i.e. ‘proper distances’, Weinberg 1972, equivalent to ‘conformal time’ if  $c = 1$ ). Since the counterexample 3-manifold used is  $T^2$ , the metric assumed is flat, i.e.,  $\Omega_0 + \lambda_0 \equiv 1$ , where  $\Omega_0$  is the present value of the density parameter and  $\lambda_0$  is the present value of the dimensionless cosmological constant.

## 2 Method

### 2.1 The Identified Circles Principle

The identified circles principle was first published by Cornish, Spergel & Starkman (1996; 1998b), and can be briefly resumed as follows.

The set of multiply topologically imaged points can be generated by considering copies of the observer in the covering space placed at distances less than the horizon diameter from the observer. The intersection of the two last scattering surfaces (spheres) of the observer and a copy of the observer is a circle. But, since the copy of the observer is physically identical to the observer, what in the covering space appears to be two observers looking at one circle is equivalent to one observer looking at two circles.

If the radiation from the surface of last scattering is isotropic, then the temperature fluctuations around the one circle seen by the ‘two observers’ are identical, apart from measurement uncertainty, and foreground contributions to the observed temperatures. Hence, the temperature fluctuations around the two circles seen by the one observer should also be identical.

It should be noted that for this reasoning to be valid (or for the reasoning behind pertur-

bation assumption based methods to be valid) for four-year COBE data, the averaging of temperature estimates over the two transverse sizes ( $\sim 1000h^{-1}$  Mpc) of the three-dimensional plasma patch which generates a COBE ‘pixel’ would need to compensate for its thinness ( $\sim 10h^{-1}$  Mpc) in the radial direction, since the latter might lead to unexpected effects from the  $10h^{-1}$  Mpc scale. See fig. 14 and Section 5.3.2 of Luminet & Roukema (1999) for an illustration and brief discussion of this question.

It is assumed here that this averaging is valid, as was assumed implicitly by authors making calculations using perturbation statistic based methods (e.g. de Oliveira-Costa et al. 1996; Levin et al. 1998). If it were *not* valid, then the published calculations claiming to show that  $2r_{\text{inj}} > 8R_H/10$  for flat multiply connected universe models would be invalid, and would be disproved without requiring an explicit counterexample 3-manifold. Since the gravitational potential generating the naïve Sachs-Wolfe effect is expected to be reasonably smooth on a scale of  $1000h^{-1}$  Mpc, it is reasonable to suppose that the averaging process is valid, though this has not yet been studied rigorously in the context of cosmic topology.

It should be noted, in particular, that the averaging should overcome having to consider the Doppler contribution to the temperature fluctuations, which is not isotropic.

## 2.2 ‘Good’ Null Hypotheses

As has already been pointed out by several authors (Starobinsky 1993; Fang 1993; de Oliveira-Costa et al. 1996), a small  $T^2$  universe would cause an approximate symmetry in the CMB if the CMB temperature fluctuations were only caused by the naïve Sachs-Wolfe effect. This can be thought of in terms of the identified circles by realising that the planes of the matched circles are all parallel to the long  $T^2$  axis. All vectors between identified points are orthogonal to the long axis. Hence, along any circle on the surface of last scattering which is centred on (orthogonal to) the long axis, many pairs of identical temperatures should exist.

A fast method of finding a ‘good’  $T^2$  hypothesis for a given value of  $2r_{\text{inj}}$  is therefore to find the angular position of the long axis which maximises

the auto-correlation statistic  $S_{T^2}(l^{\text{II}}, b^{\text{II}})$ , defined

$$S_{T^2}(l^{\text{II}}, b^{\text{II}}) \equiv \frac{\left\langle 2 \left( \frac{\delta T}{T} \right)_i \left( \frac{\delta T}{T} \right)_j \right\rangle}{\left\langle \left[ \Delta \left( \frac{\delta T}{T} \right) \right]_i^2 + \left[ \Delta \left( \frac{\delta T}{T} \right) \right]_j^2 \right\rangle} \quad (1)$$

where  $\left( \frac{\delta T}{T} \right)_i$  and  $\left( \frac{\delta T}{T} \right)_j$  are the temperature fluctuations in two celestial positions  $(i, j)$  at equal angles from the long  $T^2$  axis in the direction  $(l^{\text{II}}, b^{\text{II}})$ , (i.e. along a circle orthogonal to the long  $T^2$  axis) and  $\Delta \left( \frac{\delta T}{T} \right)_i$  and  $\Delta \left( \frac{\delta T}{T} \right)_j$  are the corresponding one standard deviation measurement uncertainties. If the  $T^2$  hypothesis with a long axis at  $(l^{\text{II}}, b^{\text{II}})$  were correct, then some of these pairs  $(i, j)$  would denote matched pixels, but many others would not. If the Universe were simply connected, then none of the pairs would denote matched pixels.

The highest few values of  $S_{T^2}$  define the long axes of ‘good’  $T^2$  hypotheses. Since this symmetry statistic is only an approximate indicator of multiple connectedness, combining matched pairs and unmatched pairs, the short axes need to be chosen and the identified circles principle applied in order to see if these long axes really do imply good multiply connected models. A range of orientations of the two short axes (assumed to be orthogonal to each other and to the long axis) needs to be considered for long axis positions close to those suggested by the  $S_{T^2}$  statistic. An identified circle statistic is used to test each possibility (Sect. 2.3).

It is found here that this procedure is sufficient to find a ‘good’ null hypothesis, as quantified below.

## 2.3 Null Hypothesis Testing

To see if the measured temperature fluctuations are consistent with multiple topological imaging, the null hypothesis that temperatures on corresponding ‘pixels’ are equal to within observational error is considered.

The null hypothesis is tested by considering the difference in the temperature fluctuations in two corresponding ‘pixels’ on matched circles to be a random realisation of a Gaussian distribution centred on zero with a width determined by the uncertainties of the measurements in the two pixels. By normalising the difference for each pair by the uncertainty in that difference, the full set of pairs of multiply imaged pixels is combined to

form a large sample of a single distribution  $\{d_{ij}\}$ , which should have a mean of zero and a standard deviation of unity if the null hypothesis is correct.

The normalised difference is defined

$$d_{ij} \equiv \frac{\left[ \left( \frac{\delta T}{T} \right)_i - \left( \frac{\delta T}{T} \right)_j \right]}{\sqrt{\left[ \Delta \left( \frac{\delta T}{T} \right) \right]_i^2 + \left[ \Delta \left( \frac{\delta T}{T} \right) \right]_j^2}} \quad (2)$$

with the same notation as above, except that in this case *every* pair  $(i, j)$  corresponds to hypothetically identical pixels. The standard deviation  $\sigma$  is defined by

$$\sigma^2(r) \equiv \langle d_{ij}^2 \rangle \quad (3)$$

and the mean difference is

$$d \equiv \langle d_{ij} \rangle \quad (4)$$

where  $(i, j)$  vary over all pairs of points on matched circle pairs.

The observed distribution  $d_{ij}$  is compared with a Gaussian distribution of mean zero and standard deviation unity via a Kolmogorov-Smirnov (KS) test. Since the circles oversample the COBE data set, i.e. there are only  $\sim 300$  independent pixels, or  $\sim 150$  independent pixel pairs, in the COBE data set (for a  $\pm 20^\circ$  galactic cut and  $10^\circ$  resolution), a subset of less than  $\sim 150$   $d_{ij}$  independent values exists (since not all points above galactic latitudes of  $20^\circ$  are on identified circles). An upper bound on the KS probability  $P$  that the observed distribution is consistent with the null hypothesis can be provided by using the full set of circles but using  $N = 150$  in the probability estimate ( $P_{\text{all}}$ ), while a lower bound (and more accurate estimate) can be provided by choosing an evenly spaced subset of the circles containing  $\sim 150$   $d_{ij}$  values, which removes most of the correlated pixels ( $P_{\text{subs}}$ ).

For completeness, the statistic of Cornish, Spergel & Starkman (1998b) should be mentioned. This is essentially a two-point autocorrelation function normalised by the variance per pixel [eq. (2) of Cornish, Spergel & Starkman], defined

$$S \equiv \frac{\left\langle 2 \left( \frac{\delta T}{T} \right)_i \left( \frac{\delta T}{T} \right)_j \right\rangle}{\left\langle \left( \frac{\delta T}{T} \right)_i^2 + \left( \frac{\delta T}{T} \right)_j^2 \right\rangle} \quad (5)$$

again using the same notation, where  $i$  and  $j$  denote matched pixels. Note that this differs from  $S_{T^2}$  defined in Sect. 2.2.

## 2.4 Integrated Sachs-Wolfe Effect and Other ‘Noise’

Previous authors comparing flat multiply connected 3-manifolds to statistics derived from COBE maps have ignored the ISW effect. These foreground temperature fluctuations are generally present on large scales, except in the special case of an  $\Omega_0 = 1, \lambda_0 = 0$  universe.

Due to the lack of sufficient knowledge of the three-dimensional map of the gravitational potential from the observer to a redshift of  $z \sim 2$ , an observationally based estimation of the ISW effect would require considerable model dependent extrapolation from observational data. However, statistical, theoretical estimates of the ISW effect can be made.

The observed values of  $\delta T/T$  can then be treated as estimates of the NSW effect which contain systematic uncertainties of the order of magnitude of the ISW effect. The  $\delta T/T$  contributions of the ISW effect in two multiply imaged pixels should not be any more correlated with one another than any non-multiply imaged pixels. (‘Multiply imaged’ refers here only to the surface of last scattering.) Hence, the ISW components of the  $\delta T/T$  values can be approximated as noise.

From fig. 1 of Crittenden & Turok (1996), it is shown that for a value of  $\lambda_0 \approx 0.8$  (and  $h = 0.7$ , both values of which are close to observationally favoured values), the ISW contribution to  $\delta T/T$  values can be nearly as much as the NSW contribution on large scales. This can be parametrised for the present purposes by

$$x^2 \equiv \frac{\left\langle \left( \frac{\delta T}{T} \right)_{\text{ISW}}^2 \right\rangle}{\left\langle \left( \frac{\delta T}{T} \right)_{\text{NSW}}^2 \right\rangle + \left\langle \left( \frac{\delta T}{T} \right)_{\text{ISW}}^2 \right\rangle}, \quad (6)$$

so that the temperature uncertainties can be re-estimated as

$$\left[ \Delta \left( \frac{\delta T}{T} \right) \right]^2 \equiv \left[ \Delta \left( \frac{\delta T}{T} \right) \right]_{\text{obs}}^2 + x^2 \left\langle \left( \frac{\delta T}{T} \right)^2 \right\rangle \quad (7)$$

where  $[\Delta (\delta T/T)]_{\text{obs}}^2$  is the measurement uncertainty.

The NSW and ISW are assumed to be uncorrelated with one another, since gravitational structures at  $z < 2$  and  $z \approx 1100$  should not be significantly cross-correlated for a simply connected model, and should only (at most) be very marginally cross-correlated in the multiply connected case.

For a simply connected model, this is simply because the distances are very large, so cross-correlations would be very weak. For a multiply connected model, a single density perturbation will in many cases make  $\delta T/T$  contributions to the ISW at differing redshifts, which, if it were somehow possible to separate these by labelling them by their redshifts, would contribute multiple topological ‘images’ in differing directions and at differing redshifts to a CMB map, where an ‘image’ is the integral over a short redshift interval of the time varying gravitational potential in some direction. However, the absence of such ‘redshift labels’ and resulting projection (integration) of this effect over a wide range in redshift is likely to make both the resulting auto-correlations and the cross-correlations with NSW contributions (at the surface of last scattering) small in amplitude. Hence, a conservative modelling of the ISW is to treat it as noise which is uncorrelated with the NSW.

A range of values  $0.0 < x^2 < 0.6$  is considered. This can represent the ISW effect and/or systematic uncertainties not otherwise taken into account. Because the signal to noise ratio of the smoothed data is  $\sim 2$ , a value of  $x^2 = 0.5$  would correspond to assuming that the total random plus systematic uncertainties are about twice ( $1 + 0.5 \times 2 = 2$ ) the random uncertainties as calculated by the COBE team.

## 2.5 Observations

The COBE DMR four years’ observational data (Bennett et al. 1994) are used as recommended by the COBE team. These are made available (web address in acknowledgments) as dipole subtracted, foreground corrected ‘DMR Analysed Science Data Sets’ (hereafter, ASDS). The ASDS corrected for galactic emission by the ‘combination’ technique of removing synchrotron, dust and free-free emission is used, where the weights used by the COBE team for combining the 31GHz, 53GHz and 90GHz maps are  $-0.49$ ,  $1.42$  and  $0.18$  respectively

Data between galactic latitudes of  $-20^\circ$  and  $+20^\circ$  are not considered.

Since the data set provided is oversampled, a smoothing by a Gaussian of  $10^\circ$  full width half maximum (FWHM) (differences between two beams of  $7^\circ$  were measured by the DMR, i.e. Differential Microwave Radiometer) is necessary.

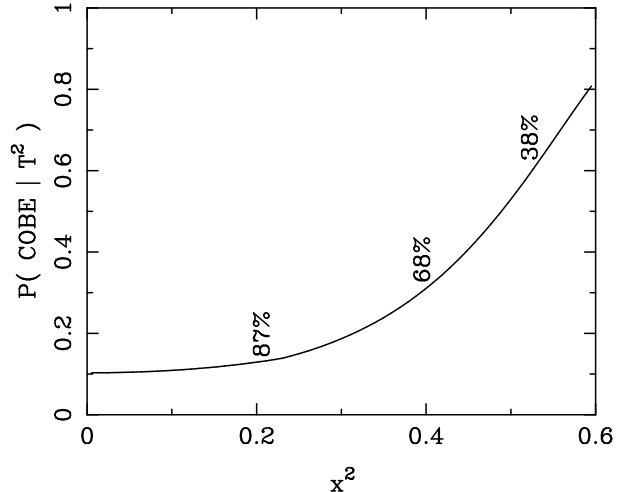


Figure 1: Probability,  $P_{\text{subs}}$  given the small  $T^2$  model indicated in Table 2 as a null hypothesis, that the differences around matched circles in the COBE data are simply due to random error, integrated Sachs-Wolfe contributions and other systematic (or random) error, where  $x^2$  [eq. (6)] represents the contribution of the latter two. Some significance levels for rejection of the hypothesis are labelled at appropriate points. A rejection of 95% (which would correspond to a two-tailed Gaussian rejection at two standard deviations if the probability distribution were Gaussian) is not attained, even for  $x^2 = 0$  (no ISW contribution), where  $1 - P = 92\%$ .

## 3 Results

Calculation of the  $S_{T^2}$  symmetry statistic for the ASDS map (with a  $10^\circ$  FWHM smoothing) results in a list of ‘good’ possibilities for the orientation of the long axis of a  $T^2$  model. The three positions with the highest values of  $S_{T^2}$  are listed in Table 1. The second and third positions are approximate antipodes, suggesting that a ‘good’  $T^2$  candidate should have a long axis close to these two positions. This indeed is the case.

A search of orientations within  $\sim 5^\circ$  of these long axis positions for various possibilities of or-

Table 1: Sky positions of long axis for ‘good’  $T^2$  hypotheses based on maximising the symmetry statistic  $S_{T^2}$  [eq. (1)]. Galactic longitude, latitude and  $S_{T^2}$  are listed. Adjacent pairs  $(i, j)$  are excluded from the  $S_{T^2}$  values shown, in order to decrease noise from close pixels.

$l^{\text{II}}$	$b^{\text{II}}$	$S_{T^2}$
$329^\circ$	$-42^\circ$	0.23
$282^\circ$	$32^\circ$	0.22
$104^\circ$	$-38^\circ$	0.21

thogonal short axes was performed. A difference set around matched circles  $\{d_{ij}\}$  and a Kolmogorov-Smirnov comparison of  $\{d_{ij}\}$  with a Gaussian distribution (of mean zero and standard deviation unity) were calculated for the different orientations.

A ‘good’ 3-manifold hypothesis found by this procedure is defined in Table 2. KS probabilities that the COBE data differences in supposedly matched pixels can occur, given the null hypothesis that the multiple topological imaging due to the 3-manifold chosen occurs, are also indicated in Table 2 for the full set of circles ( $P_{\text{all}}$ , which is an overestimate of  $P$ ) and for a subset ( $P_{\text{subs}}$ , which is a slight underestimate of  $P$ , but a better estimate than  $P_{\text{all}}$ ). An ISW/systematic error contribution of  $x = 0.3$  is assumed.

It is clear from Table 2 that this  $T^2$  model is not significantly rejected, i.e. that it is consistent with the COBE data.

Significance levels at which to reject the hypothesis are shown in Fig. 1 as a function of  $x$ , i.e. as a function of the contribution from the ISW and/or otherwise unaccounted for systematic errors. Since the value of  $\sigma$  is not much greater than unity (e.g.  $\sigma = 1.6$  for  $x^2 = 0.3$ , see Table 2), it is unsurprising that the hypothesis cannot be significantly rejected.

Fig. 1 shows that even if the COBE team’s estimates of the uncertainties are taken to include all random and systematic error and the ISW is ignored, i.e.  $x^2 = 0$ , the model is still rejected at only 92%, i.e. less than what is considered a high significance level.

What are the actual values of the temperature fluctuations along the identified circles? The identified circles for the  $T^2$  model are shown in Fig. 2, for  $x^2 = 0.3$ . The values and overall features of  $\delta T/T$  along the matched circles are not, in general, significantly different, apart from one section of the panel for  $(i, j) = (3, 0)$ .

Fig. 3 shows the COBE map in polar projection, in the  $T^2$  model coordinates, with some examples of the matched circles indicated. As explained in Sect. 2.2, an approximate circular symmetry can be expected around the long axis of a  $T^2$  model. Visual inspection of Fig. 3 suggests that the ‘northern’ hemisphere does have some circular symmetry, though circular symmetry is less obvious in the ‘southern’ hemisphere.

## 4 Discussion and Conclusions

Whereas flat multiply connected models were supposed to be excluded by COBE data for  $2r_{\text{inj}} \leq 0.4(2R_H)$ , a simple flat  $T^2$  model of  $2r_{\text{inj}} = 0.1(2R_H)$  with long and short axes at  $(l^{\text{II}}, b^{\text{II}}) = (280^\circ, 37.5^\circ)$ ,  $(184^\circ, 8^\circ)$  and  $(264^\circ, -51^\circ)$  respectively has been shown to be consistent with the COBE four year data.

This result does not show that *calculations* by previous authors were incorrect, but instead shows that some of the conclusions drawn from the calculations were over-extrapolated and somewhat overstated, with the risk of misinterpretation by non-specialist readers.

What are the differences between this result and previous authors’ work? The primary difference is the use of the identified circles principle rather than the use of indirect statistics.

Another difference, made possible by the use of the identified circles principle, is that direct observational consistency between hypothesis and data is tested, and reliance on simulations and assumptions on the statistics of density perturbations is avoided.

If one tried to reconstruct the three-dimensional field of density fluctuations in the fundamental polyhedron of the  $T^2$  model found here, it could be the case that their statistical properties are not quite Gaussian. However, this implication would *not* violate the majority of COBE analyses showing that the COBE data are consistent with Gaussianity, since, by construction, such a three-dimensional field would be directly consistent with the COBE map itself. [The same argument applies for the results of authors who find evidence of non-Gaussianity (Ferreira et al. 1998; Pando et al. 1998).]

In other words, if one calculated a statistical analysis of the temperature fluctuations corresponding to the subset of the reconstructed three-dimensional perturbation field which is restricted to the surface of last scattering, then this statistical analysis would be identical (within statistical error) to corresponding published analyses of COBE four-year data. The  $C_l$  (spherical harmonic) spectrum of the  $T^2$  solution found here is that of fig. 4 of Górski et al. (1996) and fig. 1 of Tegmark (1996). It is consistent with the  $C_l$  spectrum of the COBE data, since it *is* the spectrum of the COBE data.

A third difference is that the ISW is treated

Table 2: Axis positions of a 3-manifold candidate found close to a long axis position listed in Table 1, where the long axis ( $Z_{T_2}$ ) is larger than the horizon diameter  $2R_H$  and  $2r_{\text{inj}} \equiv 2R_H/10$  is the length of the two short axes ( $X_{T_2}$ ,  $Y_{T_2}$ ). The KS probability of finding the observed temperature differences given the 3-manifold as a null hypothesis is  $P_{\text{all}}$  or  $P_{\text{subs}}$ , depending on whether the full set of circles (where  $N = 150$  independent pairs are assumed) or an evenly spaced subset of  $N = 138$  pairs of circles, respectively, is used. An ISW/systematic noise contribution of  $x^2 = 0.3$  [eq. (6)] is adopted. Statistics  $\sigma$ ,  $d$  and  $S$  are defined in eqs (3), (4) and (5) respectively.

long ( $Z_{T_2}$ )		short ( $X_{T_2}$ )		short ( $Y_{T_2}$ )		$P(\text{all})$	$P(\text{subs})$	$\sigma$	$d$	$S$
$l^{\text{II}}$	$b^{\text{II}}$	$l^{\text{II}}$	$b^{\text{II}}$	$l^{\text{II}}$	$b^{\text{II}}$					
280	37.5	184	8	264	-51	0.40	0.19	1.61	-0.006	0.21

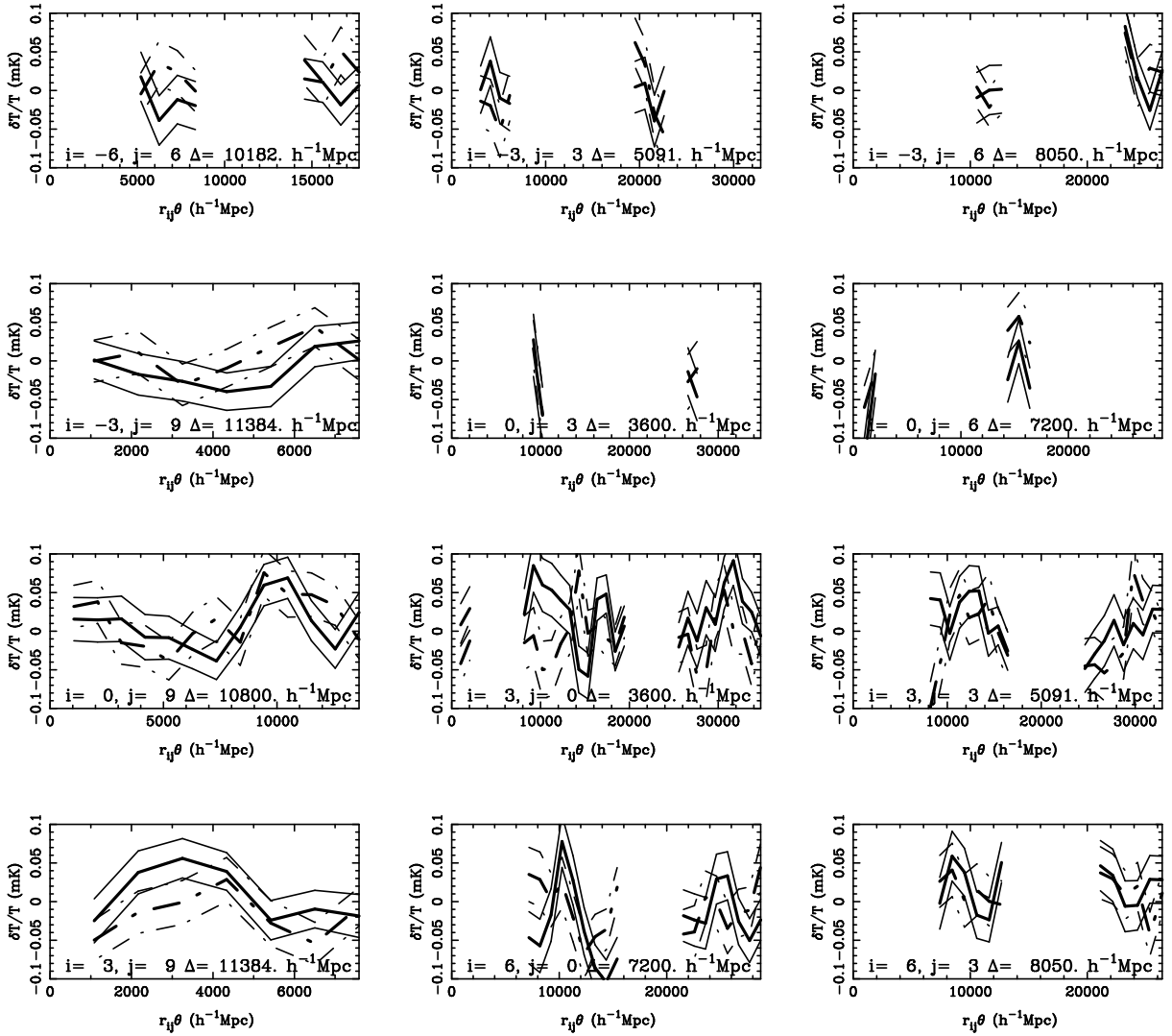


Figure 2: Temperature fluctuations in four year COBE DMR data around a subset of identified circles in the CMB, in the covering space for  $\Omega_0 + \lambda_0 = 1$ , for a  $T^2$  universe having  $2r_{\text{inj}} = 2R_H/10$  and oriented as indicated in Table 2, shown against the distance around each circle assuming  $(\Omega_0 = 1, \lambda_0 = 0)$ . Thick lines are  $\delta T/T$  and thin lines are  $\delta T/T \pm \Delta(\delta T/T)$  uncertainties for  $x = 0.3$ , i.e. including a component for the ISW effect ( $\Omega_0 < 1, \lambda_0 = 1 - \Omega_0$ ) and/or unaccounted for systematic error. Solid and dot-dashed lines distinguish the members of each circle pair. The horizontal length of each panel is the circle circumference if  $(\Omega_0 = 1, \lambda_0 = 0)$ . Circles are labelled  $(i, j)$ , where each circle lies in a plane halfway between the observer and her/his topological image at  $i(2R_H/10)\mathbf{e}_x + j(2R_H/10)\mathbf{e}_y$  and its matching circle is at  $(-i, -j)$ , where  $\mathbf{e}_x$  and  $\mathbf{e}_y$  are unit vectors in the two short directions. The distance between a circle and its match is indicated here by  $\Delta$ . Galactic latitudes with  $|b^{\text{II}}| < 20^\circ$  are excluded.

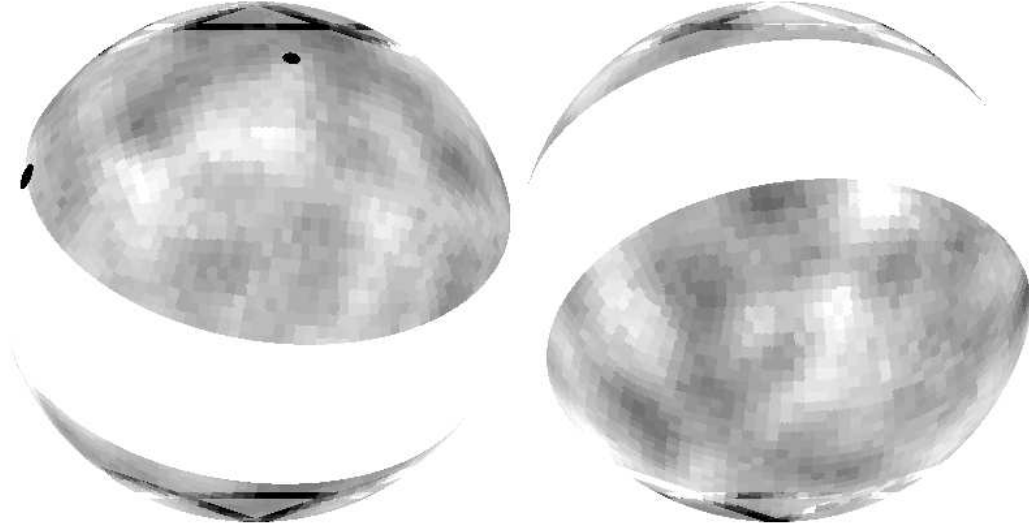


Figure 3: COBE DMR  $10^\circ$  smoothed ‘combined’ ASDS map of  $\delta T/T$  in polar projection, in coordinates of the  $T^2$  model. The  $Z_{T_2}$  axis points ‘north’ and ‘south’, i.e. is orthogonal to the plane of the page and is located at the centres of the left hand and right hand images. The  $X_{T_2}$  axis is horizontal and the  $Y_{T_2}$  axis is vertical, both are in the plane of the page. The projection is rectilinear, so that identified circles project to straight lines. The left hand hemisphere consists mostly of the north galactic hemisphere, and black spots are marked to show the north galactic pole and a point close to the galactic centre ( $l^{\text{II}} = 0, b^{\text{II}} = 20^\circ$ ). Along the galactic cut ( $\pm 20^\circ$ ), galactic longitude increases from  $\approx 0^\circ$  to  $\approx 360^\circ$  from right to left. The identified circles for  $(i, j) = (-3, 9), (0, 9)$  and  $(-3, 9)$  are highlighted by multiplying the  $\delta T/T$  values by a factor of 5.

here (in a simple but quantitative way). However, Fig. 1 shows that it is not necessary for the ISW to be dominant (greater in amplitude than the NSW component) for the 3-manifold to be consistent with the COBE data. An ISW component from half to equal the amplitude of the NSW component, i.e. where  $0.33 \leq x^2 \leq 0.5$ , implies  $80\% \geq 1 - P \geq 50\%$  rejection levels of the 3-manifold respectively, i.e. implies that the 3-manifold is consistent with the COBE data even though the ISW component is weak. Inclusion of an ISW component in the perturbation statistic methods cited above would modify the results of those calculations, but is unlikely that it would invalidate them.

It could also be argued that there is a philosophical difference relative to the simulation based results. This is expressed statistically and is sometimes titled the ‘cosmic variance’ argument.

The analyses using simulations quote statistical confidence levels relating to an ensemble of ‘observable’ universes (where an observable universe is equivalent to the space up to our own horizon), either theoretical observable universes or different samples of the one physical Universe which are observable in principle if one waits many Hubble times. It is then assumed by the Copernican principle that parameters of our observable Universe

should be within a few standard deviations of the mean of any measurable parameter.

However, if the Universe is observably small, then there exist no other samples of observable universes, and the theoretical properties are unlikely to be exactly identical to those generally assumed.

On the other hand, the confidence levels in this study relate only to measurement uncertainties in the  $\delta T/T$  values, plus extra allowance for the integrated Sachs-Wolfe effect (for a high value of the cosmological constant  $\lambda_0 = 1 - \Omega_0$ ) and possible other systematic measurement uncertainties. The cosmic variance argument is not invoked.

Although it has been shown that a  $2r_{\text{inj}} = 2R_H/10$  multiply connected model of the Universe which is consistent with the COBE four year data can easily be found, it is *not* the theme of this paper to claim that this should be considered a strong candidate for the 3-manifold of the Universe. Finding one counterexample is not the same task as finding the best counterexample, nor is it anywhere near sufficient to reject the simple connectedness hypothesis. For example, as in the case of other authors,  $T^2$  models are only considered for which the faces of the fundamental polyhedron are mutually orthogonal.

Nevertheless, the  $T^2$  model found could be



Table 3: Axis positions, statistics and null hypothesis probabilities, as for Table 2, for a  $T^2$ ,  $2r_{\text{inj}} = 2R_H/10$  model strongly rejected using the identified circles principle, in spite of the presence of a strong ISW effect, with  $x^2 = 0.6$ .

long ( $Z_{T_2}$ )		short ( $X_{T_2}$ )		short ( $Y_{T_2}$ )		$P(\text{all})$	$P(\text{subs})$	$\sigma$	$d$	$S$
$l^{\text{II}}$	$b^{\text{II}}$	$l^{\text{II}}$	$b^{\text{II}}$	$l^{\text{II}}$	$b^{\text{II}}$					
191	-57.5	325	-24	244	21	0.002	0.001	1.7	-0.25	-0.02

considered as a useful working hypothesis, or as a candidate 3-manifold, for use in working carefully through the details of methods, analyses or searches for systematic errors, both for two-dimensional (CMB) and three-dimensional [catalogues of collapsed luminous objects (Lehoucq et al. 1996; Roukema 1996; Roukema & Edge 1997)] studies.

The reader should be reminded that application of the identified circles principle is powerful enough to reject small universe hypotheses with the COBE four-year observational data, even in the presence of a strong ISW effect.

For example, use of the  $S_{T^2}$  test as above (Sect. 2.2) to find examples of ‘bad’  $T^2$  hypotheses (by the most negative values of  $S_{T^2}$ ) and followup by null hypothesis testing (as in Sect. 2.3) leads to the results in Table 3. If the  $T^2$  model defined in Table 3 were correct, then even with  $x^2 = 0.6$  [eq. (6)], i.e. with a large contribution of the ISW effect which hides a lot of the signal from the surface of last scattering, then the probability of obtaining the COBE observations is  $P(\text{subs}) = 0.001 \lesssim P < P(\text{all}) = 0.002$ . In other words, the hypothesis is rejected at the  $99.8\% < 1 - P$  level.

Future uses of the present study may help to suggest ways of searching for systematic errors in CMB data, and trying to find ways of avoiding these.

For example, the seriousness of contamination by the galactic plane for cosmic topology studies is clear in Fig. 3. A large fraction of pixel pairs which could contribute to strengthening or weakening of a  $T^2$  hypothesis are invalid because one or the other of the pixels in the pair lies close to the galactic plane.

Other topologically non-trivial 3-manifolds could obviously have similar problems.

Another possibility would be to follow up the circular symmetry evident in Fig. 3. If there were a valid physical argument explaining why

the northern galactic hemisphere COBE measurements had a circular symmetry imposed, then that could refute this particular counterexample. This would imply that another would have to be sought based on the new effect, but would also imply an effect which would need to be taken into account for analyses of MAP and Planck Surveyor data — whether for cosmic topology or other purposes.

Alternatively, if there were a valid physical argument explaining why the southern galactic hemisphere COBE map (but not the northern hemisphere) contained a systematic error of the order of magnitude of the measurement error already present, then the specific  $T^2$  model found here would be considerably strengthened.

In the absence of such a physical argument, the  $T^2$  model found simply remains a counterexample to the claimed ‘constraints’.

## Acknowledgments

Helpful discussions and encouragement from Ubi Wichoski, Suketu Bhavsar and Tarun Souradeep were greatly appreciated. Use was made of the COBE datasets ([http://www.gsfc.nasa.gov/astro/cobe/cobe\\_home.html](http://www.gsfc.nasa.gov/astro/cobe/cobe_home.html)) which were developed by NASA’s Goddard Space Flight Center under the guidance of the COBE Science Working Group and were provided by the NSSDC.

## References

- Aurich R., 1999, ApJ, 524, 497 (arXiv:astro-ph/9903032)
- Bennett, C. L., et al., 1992, ApJ, 396, L7
- Bennett, C. L., et al., 1994, ApJ, 436, 423
- Blanlœil V., Roukema B. F., (editors) 1999, proceedings of *Cosmological Topology in Paris 1998*,

- 14 Dec 1998, Obs. Paris, <http://www.iap.fr/users/roukema/CTP98/programme.html>
- Bond J. R., Pogosyan D., Souradeep T., 1998, *ClassQuantGra*, 15, 2573 (arXiv:astro-ph/9804041)
- Chiba M., Yoshii Y., 1997, *ApJ*, 489, 485
- Cornish N. J., Spergel D. N., 1999, arXiv:astro-ph/9906401
- Cornish N. J., Spergel D. N., Starkman G. D., 1996, arXiv:gr-qc/9602039
- Cornish N. J., Spergel D. N., Starkman G. D., 1998a, *Phys.Rev.D*, 57, 5982 (arXiv:astro-ph/9708225)
- Cornish N. J., Spergel D. N., Starkman G. D., 1998b, *ClassQuantGra*, 15, 2657 (arXiv:astro-ph/9801212)
- Crittenden R. G., Turok N., 1996, *PhysRevLett*, 76, 575
- de Oliveira Costa A., Smoot G. F., 1995, *ApJ*, 448, 477
- de Oliveira Costa A., Smoot G. F., Starobinsky A. A., 1996, *ApJ*, 468, 457
- Fagundes H. & Gausmann E., 1998, *PhysLettA*, 238, 235 (arXiv:astro-ph/9704259)
- Fagundes H. & Gausmann E., 1999a, in *Proceedings of the XIX Texas Symp. Rel. Astr. Cosmology*, CD-ROM version (arXiv:astro-ph/9811368)
- Fagundes H. & Gausmann E., 1999b, *PhysLettA*, 261, 235 (arXiv:astro-ph/9906046)
- Fang, L.-Z., 1993, *Mod.Phys.Lett.A*, 8, 2615
- Ferreira P. G., Magueijo J., Górski, K. M., 1998, *ApJ*, 503, L1 (arXiv:astro-ph/9803256)
- Fort B., Mellier Y., Dantel-Fort M., 1997, *A&A*, 321, 353
- Fukugita, M., Yamashita, K., Takahara, F., Yoshii, Y., 1990, *ApJ*, 361, L1
- Gomero G. I., Teixeira A. F. F., Rebouças M. J., Bernui A., 1999a, arXiv:gr-qc/9811038
- Gomero G. I., Rebouças M. J., Teixeira A. F. F., 1999b, arXiv:gr-qc/9909078
- Gomero G. I., Rebouças M. J., Teixeira A. F. F., 1999c, arXiv:gr-qc/9911049
- Górski K. M., Banday A. J., Bennett C. L., Hinshaw G., Kogut A., Smoot G. F., Wright E. L., 1996, *ApJ*, 464, L11
- Inoue K. T., 1999, *ClassQuantGra*, 16, 3071 (arXiv:astro-ph/9810034)
- Jing Y.-P., Fang L.-Z., 1994, *PhysRevLett*, 73, 1882 (arXiv:astro-ph/9409072)
- Lachièze-Rey M., Luminet J.-P., 1995, *PhysRep*, 254, 136 (arXiv:gr-qc/9605010)
- Lehoucq R., Luminet J.-P., Lachièze-Rey M., 1996, *A&A*, 313, 339
- Lehoucq R., Luminet J.-P., Uzan, J.-Ph., 1999, *A&A*, 344, 735 (arXiv:astro-ph/9811107)
- Levin J., Scannapieco E., Silk J., 1998, *Phys.Rev.D*, 58, 103516 (arXiv:astro-ph/9802021)
- Luminet J.-P., 1998, *Acta Cosmologica*, 24, (arXiv:gr-qc/9804006)
- Luminet J.-P., Roukema B. F., 1999, 'Topology of the Universe: Theory and Observations', Cargèse summer school 'Theoretical and Observational Cosmology', ed. Lachièze-Rey M., Netherlands: Kluwer, p117 (arXiv:astro-ph/9901364)
- Pando J., Valls-Gabaud D., Fang L.-Zh., 1998, *PhysRevLett*, 81, 4568 (arXiv:astro-ph/9810165)
- Perlmutter S. et al., 1999, *ApJ*, 517, 565 (arXiv:astro-ph/9812133)
- Roukema B. F., 1996, *MNRAS*, 283, 1147
- Roukema B. F., 2000, *MNRAS*, 312, 712 (arXiv:astro-ph/9910272)
- Roukema B. F., Blanlœil V., 1998, *ClassQuantGra*, 15, 2645 (arXiv:astro-ph/9802083)
- Roukema B. F., Edge A. C., 1997, *MNRAS*, 292, 105
- Sachs, R. K., Wolfe A. M., 1967, *ApJ*, 147, 73
- Schwarzschild, K., 1900, *Vier.d.Astr.Gess.*, 35, 337

- Schwarzschild, K., 1998, *ClassQuantGra*, 15, 2539 [english translation of Schwarzschild (1900)]
- Sokolov, I. Yu., 1993, *JETPLett*, 57, 617
- Starobinsky A. A., 1993, *JETPLett*, 57, 622
- Starkman G. D., 1998, *ClassQuantGra*, 15, 2529
- Stevens D., Scott D., Silk J., 1993, *PhysRevLett*, 71, 20
- Tegmark M., 1996, *ApJ*, 464, L35 W. P., 1997, *Three-Dimensional Geometry and Topology*, ed. Levy, S., Princeton, U.S.A.: Princeton University Press
- Uzan, J.-Ph., 1998, *Phys.Rev.D*, 58, 087301 (arXiv:gr-qc/9806117)
- Uzan J.-Ph., Lehoucq R. & Luminet J-P., 1999, *A&A*, 351, 766 (arXiv:astro-ph/9903155)
- Weeks J. R., 1998, *ClassQuantGra*, 15, 2599 (arXiv:astro-ph/9802012)
- Weinberg, S., 1972, *Gravitation and Cosmology*, New York, U.S.A.: Wiley
- White, M., Scott, D., Silk, J., 1994, *AnnRevA&A*, 32, 319